

Influence of forming process on three-dimensional morphology of TiB₂ particles in Al–Ti–B alloys

LI Peng-ting, LI Yun-guo, NIE Jin-feng, LIU Xiang-fa

Key Laboratory for Liquid-Solid Structural Evolution and Processing of Materials,
Ministry of Education, Shandong University, Ji'nan 250061, China

Received 21 March 2011; accepted 20 December 2011

Abstract: A series of Al–Ti–B master alloys were prepared by different preparation routes, and the TiB₂ particles in the master alloys were extracted and analyzed. It is found that the forming process has significant influence on the three-dimensional morphology of TiB₂ particles. Different preparation routes result in different reaction forms, which accounts for the morphology variation of TiB₂ particles. When the Al–Ti–B master alloy is prepared using “halide salt” route, TiB₂ particles exhibit hexagonal platelet morphology and are independent with each other. In addition, the reaction temperature almost does not have influence on the morphology of TiB₂ particles. However, TiB₂ particles exhibit different morphologies at different reaction temperatures when the master alloys are prepared with Al–3B and Ti sponge. When the master alloy is prepared at 850 °C, a kind of TiB₂ particle agglomeration forms with a size larger than 5 μm. The TiB₂ particles change to layered stacking morphology even dendritic morphology with the reaction temperature reaching up to 1200 °C.

Key words: Al–Ti–B alloy; TiB₂; forming process; three-dimensional morphology

1 Introduction

Al–Ti–B master alloys are good refiners for Al and its alloys [1–3], and Al–TiB₂ alloys can be used as composites due to good wear resistance, high tensile strength and elastic modulus [4–6]. The widely used preparation method of Al–Ti–B alloys is “halide salt” route [5–8], but it suffers several drawbacks in practice caused by the low content of B and Ti in the fluoride, such as a large amount of fluoride addition, serious pollution, and difficulty to control [2,9,10]. In recent years, extensive studies have been conducted by changing the raw materials and process. For example, YÜCEL [11] prepared a more effective Al–Ti–B master alloy by replacing KBF₄ with Na₂B₄O₇ or B₂O₃ via self-propagating high-temperature synthesis (SHS) technology.

From existing studies, it is found that different preparation routes result in different refining abilities or mechanical properties of the Al–Ti–B alloys [2, 7–13]. It is thought that the morphology of TiB₂ particles plays a

vital role in the grain refiners and composites. However, the studies of Al–Ti–B alloy were mainly focused on the morphology of TiAl₃ particles and the distribution of TiB₂ particles in previous works [7–11], and a comprehensive study on the three-dimensional morphology of TiB₂ particles in Al–Ti–B alloy has not been conducted.

In this study, Al–5Ti–1B (all compositions quoted in this work are in mass fraction unless otherwise stated) master alloys were prepared by different processes, and the TiB₂ particles in the master alloys were extracted. The influence of forming process on the three-dimensional morphology of TiB₂ particles in Al–Ti–B master alloys was studied.

2 Experimental

A series of Al–5Ti–1B master alloys were prepared by different processes (Table 1). 99% KBF₄ and K₂TiF₆, 99.8% Ti sponge, 99.7% commercial pure Al and Al–3B master alloy were used in this study. About 2 kg commercial pure Al was melted in a medium frequency

furnace and the mixed powders of KBF_4 and K_2TiF_6 were added into the melt at 850 °C or 1200 °C, which were designated as S1 and S2, respectively. After holding for 10 min, the melt was poured into an iron mould (50 mm in diameter and 25 mm in height). Another two Al–5Ti–1B master alloys were prepared with Al–3B and Ti sponge at 850 °C or 1200 °C, and were designated as S3 and S4 respectively.

Table 1 Preparation of experimental master alloys

Alloy	Raw source	Experimental temperature/°C	Alloy designation
Al–5Ti–1B	KBF_4 , K_2TiF_6	850	S1
Al–5Ti–1B	KBF_4 , K_2TiF_6	1200	S2
Al–5Ti–1B	Al–3B, Ti sponge	850	S3
Al–5Ti–1B	Al–3B, Ti sponge	1200	S4

The TiB_2 particles were extracted from all the master alloys by a special extraction method to observe the three-dimensional morphology [14]. First, the Al matrix was dissolved in a solution of 10% HCl. Next, the particles in the solution were centrifuged by a centrifugal extractor. And then the collected sediments were rinsed with distilled water and ethanol several times. The metallographic specimens were intercepted from each bottom of the samples and the phase constituent was identified by X-ray diffraction (XRD). The microstructure of the alloy and the particle morphology were examined on a field emission scanning electron microscope (FESEM) equipped with an energy-dispersive spectroscopy detector (EDS).

3 Results and discussion

3.1 Microstructure of master alloys

Figure 1 shows the microstructure of the Al–5Ti–1B master alloys prepared by “halide salt” route (S1 and S2). It can be seen that the second phase particles are relatively dispersed in Al matrix in samples S1 and S2. Furthermore, there are some block-like TiAl_3 in sample S1, as shown in Fig. 1(a). In sample S2, TiAl_3 shows stick-like morphology and is larger than that in sample S1 (Fig. 1(b)), which is attributed to the higher melting and pouring temperature.

In order to observe three-dimensional morphology and size of TiB_2 particles, the particles were extracted from the master alloys. Figures 2(a) and (b) show the morphologies of TiB_2 particles extracted from sample S1 and S2, respectively. From the corresponding XRD results in Fig. 2(a) it is found the particles mainly contain two kinds of phases: TiB_2 and TiAl_3 . The morphology of TiB_2 particles in sample S1 is hexagonal platelet, and the size is about 1 μm (with the thickness of

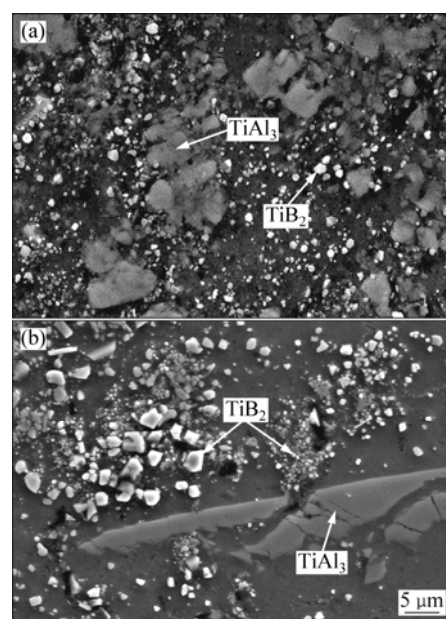


Fig. 1 FESEM images of Al–5Ti–1B master alloys prepared by “halide salt” route: (a) Sample S1; (b) Sample S2

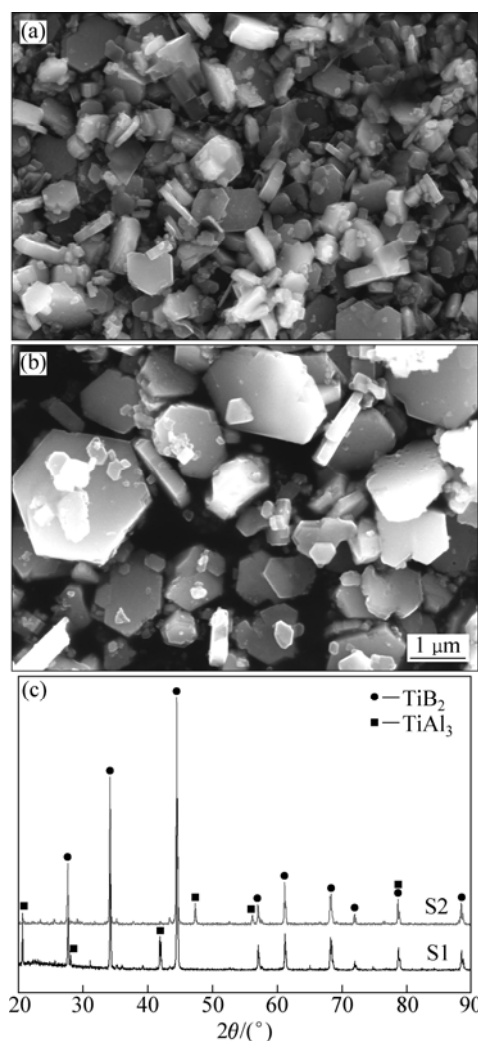


Fig. 2 FESEM images of particles extracted from samples S1 (a) and S2 (b) and XRD patterns (c)

0.2–0.5 μm). And TiB_2 particles are independent with each other. The particles in sample S2 also exhibit hexagonal platelet morphology but its size is variable, which is different with that in sample S1. Some TiB_2 particles are about 2 μm in size while others are smaller than 1 μm . The morphology of TiB_2 particles in samples S1 and S2 are almost the same, so it can be concluded that reaction temperature does not affect the morphology of TiB_2 particles in the Al–5Ti–1B master alloys prepared by “halide salt” route.

Figure 3(a) shows the SEM image of sample S3. The distribution and morphologies of TiB_2 are diverse. Some of TiB_2 are particle-like and dispersed in the Al matrix, which are similar to those in samples S1 and S2. Moreover, a lot of TiB_2 particles connect each other to form chain-like structures or agglomerate together. A TiB_2 agglomeration is magnified and analyzed by EDS, as shown in Figs. 3(b), (c) and (d). It can be seen that, in this agglomeration, the TiB_2 particles closely agglomerate and connect each other to form a whole. In the center of the TiB_2 agglomerations, unreacted AlB_2 particles are observed. The typical morphology of TiB_2 particles in sample S3 is shown in Fig. 4. The TiB_2 particles in sample S3 exist in the form of agglomeration with a size larger than 5 μm , which has been mentioned as dense agglomeration in some articles [15–18]. It is difficult for the agglomerative particles to spread in the Al melt during refinement.

Figure 5 shows the SEM image of sample S4 and

the corresponding XRD result. The master alloy mainly contains $\alpha(\text{Al})$, TiAl_3 and TiB_2 phases. From the microstructure of the alloy shown in Fig. 5(b), it can be seen that TiAl_3 particles show coarse stick-like morphology, and the distribution of TiB_2 particles also changes with the increase of the reaction temperature. Particles in sample S4 are extracted for better observation, and Fig. 6 shows the typical morphologies of TiB_2 particles. TiB_2 particles exhibit layered stacking (Fig. 6(a)) and dendritic (Fig.6(b)) morphologies, rather than independent hexagonal platelet or agglomeration. The layered stacking TiB_2 particle in Fig. 6(a) is composed of multiple thin platelets that are smaller than 0.1 μm in thickness. There are displacements between neighboring thin platelets, which helps to form a ladder structure along a certain direction [18]. The TiB_2 particle in Fig. 6(b) exhibits the dendritic morphology which is more complex than the layered stacking morphology. It can be seen that each branch of the dendritic TiB_2 particles is also layered stacking structure.

3.2 Discussion

TiB_2 crystallizes in a hexagonal lattice $P6/mmm$. It is characterized by alternating hexagonal layers of Ti and B atoms [19]. In the hexagonal structure of TiB_2 , $\{0001\}$ planes share the highest surface atomic density, which also have the lowest surface energy and the slowest growth rate. Their crystal development will be limited and the face will be shown up at last [20]. So, the TiB_2

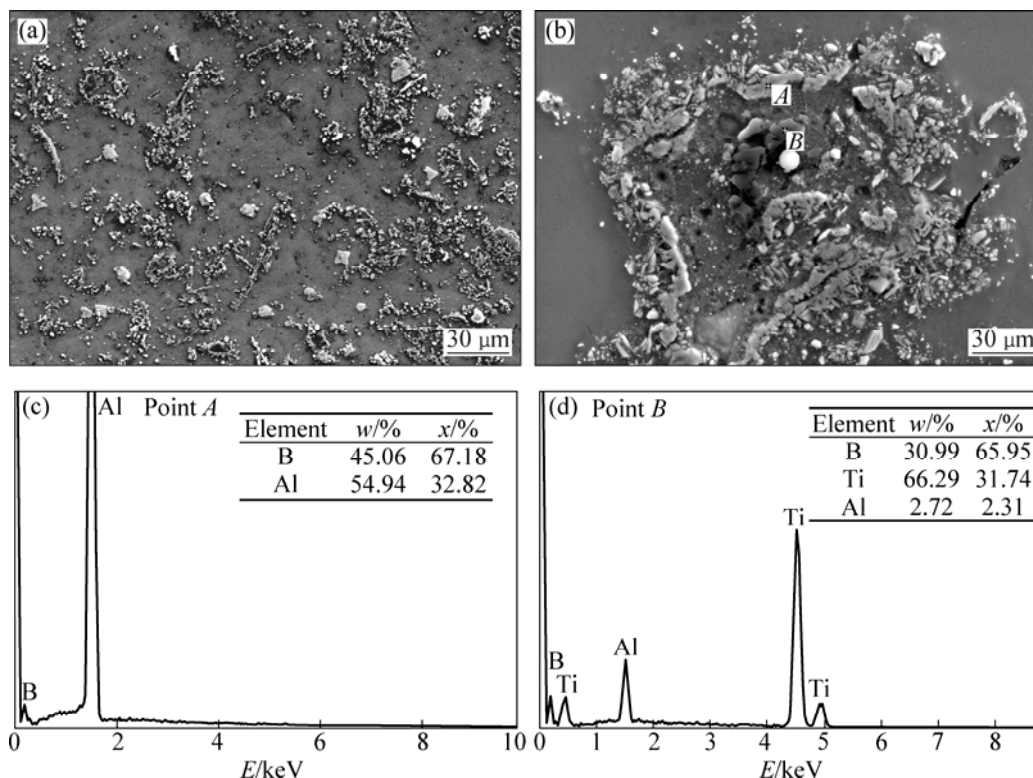


Fig. 3 FESEM images of sample S3 (a, b) and corresponding EDS results (c, d)

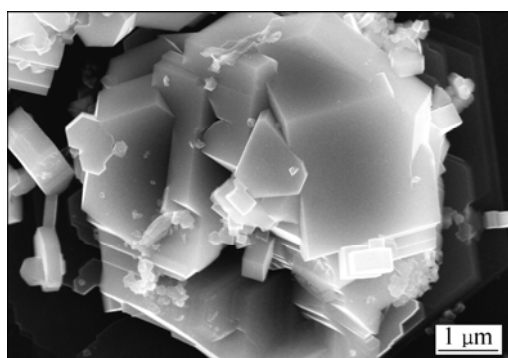


Fig. 4 FESEM image of TiB₂ agglomeration extracted from sample S3

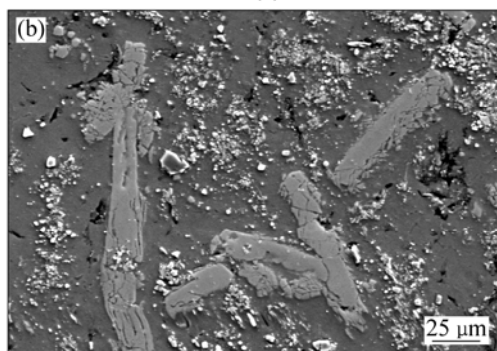
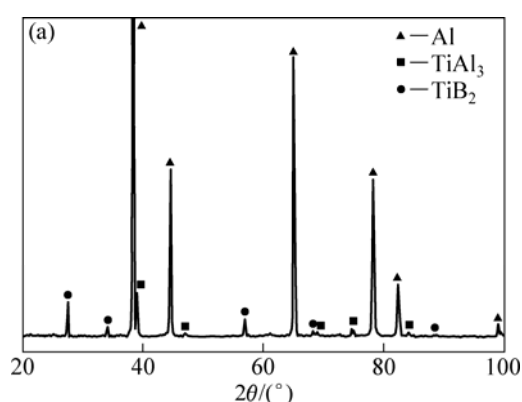


Fig. 5 XRD pattern (a) and FESEM image (b) of sample S4

particles would exhibit hexagonal morphology features. However, the three-dimensional morphologies of the TiB₂ particles in samples S1, S2, S3, and S4 are not completely identical, as shown in the results above. It is thought that this difference in particle morphology is caused by the different reactions occurring in samples S1, S2, S3, and S4 due to the different forming processes.

The formation of TiB₂ particles has been studied by many researchers [13,16]. The possible reactions in this study are

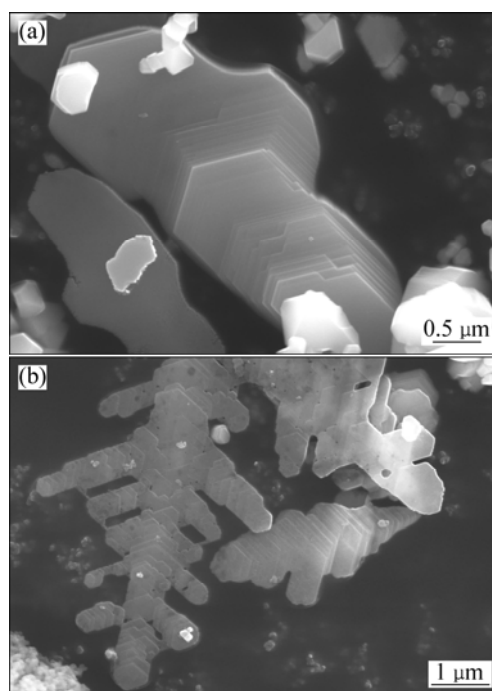
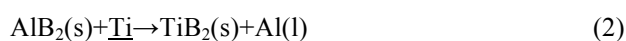
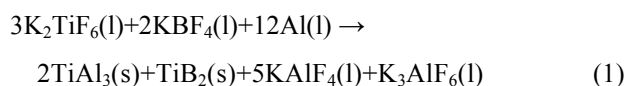


Fig. 6 SEM images showing typical morphologies of layered stacking (a) and dendritic TiB₂ particles (b) in sample S4

where $\underline{\text{B}}$ and $\underline{\text{Ti}}$ are solutes and the $\text{AlB}_2(\text{s})$ can be added by Al–B alloy or formed in the melt.

Reaction (1) is the main reaction occurring in the preparation of Al–Ti–B alloy by the “halide salt” route. When the mixed powders of KBF_4 and K_2TiF_6 are added during the preparations of S1 and S2, they float in the upper of the melt because of the low density. Reaction (1) mainly takes place in a high rate in the interface region between the mixed powders and the Al melt [17]. Figure 7(a) shows the schematic illustration of the fluoride salt/Al interfacial reaction. It should be pointed out that the concentrations of B and Ti atoms in the interface region are relatively high, which is helpful for the nucleation of TiB₂ particles. So, the nucleation of TiB₂ is intensive and many particles form in a very short time [21]. TiB₂ particles with the hexagonal morphology will form as a result of the reaction in the interface region, and fall down to the bottom of the melt when particles grow to some extent [22]. The growth of TiB₂ particles will stop after the fall. So, the TiB₂ particles in samples S1 and S2 exhibit the same morphology. It also indicates that the reaction temperature has little influence on the morphology of the TiB₂ particles in reaction (1). However, as shown in Fig. 2, the size of TiB₂ particles in sample S2 changes. Some TiB₂ particles become more than 2 μm in size while others are smaller than 1 μm. TONG et al [23] pointed out that dissolution of second phase particles in a high-temperature Al melt will occur to a certain extent, and the small particles are more likely to dissolve than big particles. It means the smallest TiB₂

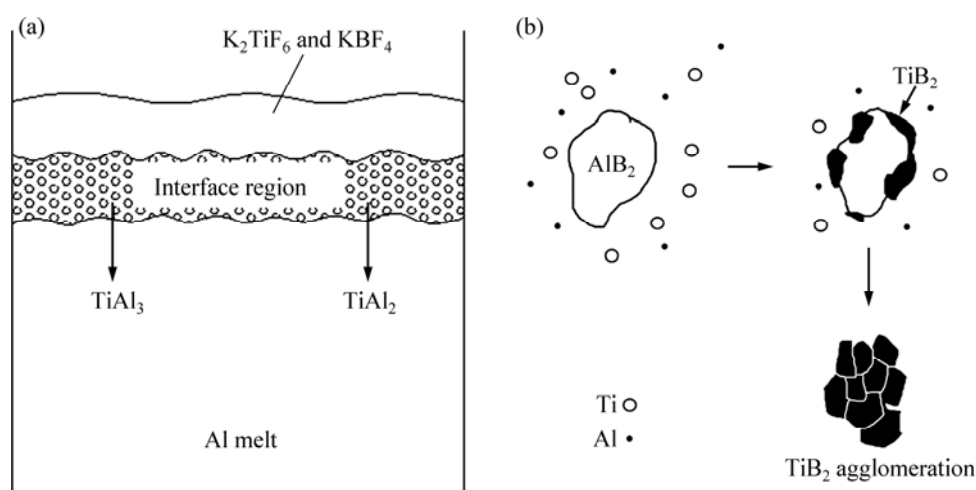


Fig. 7 Schematic illustrations of fluoride salt/Al interfacial reaction (a) and formation of TiB_2 particle agglomeration (b) in sample S3

particles nucleated in situ-reaction process re-dissolve into the high-temperature melt, and the amount of solute B is large so that the melt may be over-saturated during cooling process. It is much easier for solute Ti and B to precipitate on the surface of nucleated TiB_2 particles, because heterogeneous nucleation acquires less nucleation energy and lower undercooling. Therefore, the TiB_2 particles can grow larger during the solidification process. However, with the decrease of temperature, mass transport is getting more and more difficult as a result of the decrease of diffusion coefficient [24]. In some zone of the low temperature melt where solutes Ti and B are not able to diffuse to the surface of nucleated TiB_2 particles, they dissolve out as micro size TiB_2 particles. As a result, the size of the TiB_2 particles in sample S2 is variable due to the dissolution and precipitation of some TiB_2 particles at high temperature.

When the Al–Ti–B alloys are prepared using Al–3B and Ti sponge, the reaction forms change. So, the morphologies of the TiB_2 particles in samples S3 and S4 also change. As shown in Fig. 4, the TiB_2 particles in sample S3 tend to be in agglomeration. It is believed that the formation of TiB_2 agglomeration is related to the formation of B-containing compound in the reaction. Some articles [25,26] pointed out that the solubility of B in Al melt is very small at 850 °C and B mainly exists in the form of AlB_2 phase. So, it is thus proposed that TiB_2 in sample S3 forms through a reaction between solutes Ti and AlB_2 (reaction (2)). The schematic illustration of the agglomeration formation is shown in Fig. 7(b) and the mechanism is offered as follows: when Ti sponge is added, it starts to dissolve in molten Al and the solute Ti reacts with the existing AlB_2 to form the TiB_2 phase by replacing the Al atoms in the AlB_2 particles gradually. With the reaction process going, some TiB_2 particles form on the surface of AlB_2 particles, and they link with

each other closely in the subsequent growth process. TiAl_3 particles start to precipitate in the melt only when AlB_2 fully reacts and the Ti solubility limit (approximately 1.0 % at about 850 °C) is exceeded.

However, if the experiment temperature is raised to 1200 °C, the AlB_2 particles from Al–3B master alloy will dissolve. So, the solute Ti will preferentially react with B to form the TiB_2 phase during the preparation of S4, which can be expressed by reaction (3). It should be pointed out that the concentration of B atoms is low because they have dispersed in the whole melt. Under such condition, the successive growth of the TiB_2 particles is easier than particle nucleation. During the reaction process, thin hexagonal platelets form in the melt firstly. With the reduction in the concentration of atoms B and Ti, the nucleation of TiB_2 particles becomes more and more difficult. So, the surrounding B and Ti atoms will deposit on the surface of the nucleated particles, and new plates will form on the surface of the formed thin hexagonal platelets. On the other hand, some growth steps in TiB_2 particles emerge on the {0001} planes, as shown in Fig. 6. The presence of these growth steps indicates that the two-dimensional nucleation growth of the {0001} planes is favorable [27, 28]. This is possibly attributed to the higher reaction rate and atomic diffusion rate when the reaction temperature increases, leading to a higher density of defects (such as impurities and dislocations) in the TiB_2 crystal structure [28]. It implies that there will be more steps created by crystal defects for the growth unit to deposit on the {0001} planes. As a result, with the deposition of atoms B and Ti and the new steps generating, the TiB_2 particles with layered stacking even dendritic structure form in the Al melt finally.

The primary factor influencing the TiB_2 morphology can be ascribed to the forming process because it is most noticeable and easy to understand.

More profound investigations on the TiB₂ crystal growth are still in progress.

4 Conclusions

1) The forming process has significant influence on the three-dimensional morphology of TiB₂ particles in Al–Ti–B master alloys. Different preparation routes result in different reactions, which accounts for the morphology variation of TiB₂ particles.

2) TiB₂ particles exhibit hexagonal platelet morphology and are independent with each other, when the master alloy is prepared using “halide salt” route. In addition, the reaction temperature has no influence on the morphology of TiB₂ particles.

3) TiB₂ particles exhibit different morphologies at different reaction temperatures when the master alloys are prepared with Al–3B and Ti sponge. A kind of TiB₂ particle agglomeration forms with a size larger than 5 μm at 850 °C. The TiB₂ particles change to layered stacking morphology even dendritic morphology with the reaction temperature reaching up to 1200 °C.

References

- [1] MOHANTY P S, GRUZLESKI J E. Mechanism of grain refinement in aluminium [J]. *Acta Metallurgica et Materialia*, 1995, 43: 2001–2012.
- [2] KRISHNANA T S, RAJAGOPALANA P K, CUNDB B R, BOSEC D K. Development of Al–5%Ti–1%B master alloy [J]. *Journal of Alloys and Compounds*, 1998, 269: 138–140.
- [3] EASTON M A, STJOHN D H. A model of grain refinement incorporating alloy constitution and potency of heterogeneous nucleant particles [J]. *Acta Materialia*, 2001, 49: 1867–1878.
- [4] WILLIAM C. Commercial processing of metal matrix composites [J]. *Materials Science and Engineering A*, 1998, 24: 75–79.
- [5] YI H Z, MA N H, ZHANG Y J, LI X F, WANG H W. Effective elastic moduli of Al–Si composites reinforced in situ with TiB₂ particles [J]. *Scripta Materialia*, 2006, 54: 1093–1097.
- [6] TEE K L, LU L, LAI M O. In situ processing of Al–TiB₂ composite by the stir-casting technique [J]. *Journal of Alloys and Compounds*, 1999, 89–90: 513–519.
- [7] MURTI B S, KORI S A, VENKATESWARLU K, BHAT R R, CHAKRABORTI M. Manufacture of Al–Ti–B master alloys by the reaction of complex halide salts with molten aluminium [J]. *Journal of Materials Processing Technology*, 1999, 89–90: 152–158.
- [8] HAN Y F, SHU D, WANG J, SUN B D. Microstructure and grain refining performance of Al–5Ti–1B master alloy prepared under high-intensity ultrasound [J]. *Materials Science and Engineering A*, 2006, 430: 326–331.
- [9] XU Chun-xiang, LIANG Li-ping, LU Bin-feng, ZHANG Jin-shan, LIANG Wei. Effect of La on microstructure and grain-refining performance of Al–Ti–C grain refiner [J]. *Journal of Rare Earths*, 2006, 24: 596–601.
- [10] CHEN Ya-jun, XU Qing-yan, HUANG Tian-you. Refining performance and long time efficiency of Al–Ti–B–RE master alloy [J]. *The Chinese Journal of Nonferrous Metals*, 2007, 17: 1232–1239. (in Chinese)
- [11] YÜCEL B. Production of Al–Ti–B grain refining master alloys from B₂O₃ and K₂TiF₆ [J]. *Journal of Alloys and Compounds*, 2007, 443: 94–98.
- [12] WANG M X, WANG S J, LIU Z Y, LIU Z X, SONG T F, ZUO X R. Effect of B/Ti mass ratio on grain refining of low-titanium aluminum produced by electrolysis [J]. *Materials Science and Engineering A*, 2006, 416: 312–316.
- [13] YUCEL B. Production of Al–Ti–B master alloys from Ti sponge and KBF₄ [J]. *Journal of Alloys and Compounds*, 2007, 440: 108–112.
- [14] LIU C P, PAN F S, WANG W Q. Phase analysis of Al–Mn compounds in the AZ magnesium alloys [J]. *Materials Science Forum*, 2007, 546–549: 395–398.
- [15] SCHAFFER P L, DAHLE A K. Settling behaviour of different grain refiners in aluminium [J]. *Materials Science and Engineering A*, 2005, 413–414: 373–378.
- [16] EMAMY M, MAHTA M, RASIZADEH J. Formation of TiB₂ particles during dissolution of TiAl₃ in Al–TiB₂ metal matrix composite using an in situ technique [J]. *Composites Science and Technology*, 2006, 66: 1063–1066.
- [17] FJELLSTEDT J, JARFORS A E W. On the precipitation of TiB₂ in aluminum melts from the reaction with KBF₄ and K₂TiF₆ [J]. *Materials Science and Engineering A*, 2005, 413–414: 527–532.
- [18] LI P T, MA X G, LI Y G, NIE J F, LIU X F. Effects of trace C on the microstructure and refining efficiency of Al–Ti–B master alloy [J]. *Journal of Alloys and Compounds*, 2010, 503: 286–290.
- [19] TIAN D C, WANG X B. Electronic structure and equation of state of TiB₂ [J]. *Journal of Physics: Condensed Matter*, 1992, 4: 8765–8772.
- [20] ABDEL-HAMID A A, HAMAR-THIBAUT S, HAMAR R. Crystal morphology of the compound TiB₂ [J]. *Journal of Crystal Growth*, 1985, 71: 744–750.
- [21] JHA A, DOMETAKIS C. The dispersion mechanism of TiB₂ ceramic phase in molten aluminium and its alloys [J]. *Materials and Design*, 1997, 18: 297–301.
- [22] SCHAFFER P L, ARNBERG L, DAHLE A K. Segregation of particles and its influence on the morphology of the eutectic silicon phase in Al–7 wt.% Si alloys [J]. *Scripta Materialia*, 2006, 54: 677–682.
- [23] TONG X C, FANG H S. Al–TiC composites in situ-processed by ingot metallurgy and rapid solidification technology: Part I. Microstructural evolution [J]. *Metallurgical and Materials Transactions A*, 1998, 29: 875–891.
- [24] WU Q, LI C S, TANG H. Surface characterization and growth mechanism of laminated Ti₃SiC₂ crystals fabricated by hot isostatic pressing [J]. *Applied Surface Science*, 2010, 256: 6986–6990.
- [25] FJELLSTEDT J, JARFORS A E W, SVENDSEN L. Experimental analysis of the intermediary phases AlB₂, AlB₁₂ and TiB₂ in the Al–B and Al–Ti–B systems [J]. *Journal of Alloys and Compounds*, 1999, 283: 192–197.
- [26] WANG X M. The formation of AlB₂ in an Al–B master alloy [J]. *Journal of Alloys and Compounds*, 2005, 403: 283–287.
- [27] SONG M S, HUANG B, HUO Y Q, ZHANG S G, ZHANG M X, HU Q D, LI J G. Growth of TiC octahedron obtained by self-propagating [J]. *Journal of Crystal Growth*, 2009, 311: 378–382.
- [28] JIN S B, SHEN P, ZOU B L, JIANG Q C. Morphology evolution of TiC_x grains during SHS in an Al–Ti–C system [J]. *Crystal Growth & Design*, 2009, 9: 646–649.

合成过程对 Al-Ti-B 合金中 TiB₂ 粒子三维形貌的影响

李鹏廷, 李云国, 聂金凤, 刘相法

山东大学 材料液固结构演变与加工教育部重点实验室, 济南 250061

摘 要: 通过不同工艺制备出一系列 Al-Ti-B 中间合金, 并利用相提取工艺对合金中的 TiB₂ 粒子进行提取和分析。研究表明: 合成过程对 TiB₂ 粒子的三维形貌有显著的影响, 不同的制备工艺会导致不同的反应路径, 并最终影响 TiB₂ 粒子的形貌。利用氟盐法制备的 Al-Ti-B 中间合金中的 TiB₂ 粒子呈现相互独立的六角板块状形貌, 且反应温度不会对 TiB₂ 粒子的形貌产生影响。然而, 利用 Al-3B 中间合金和海绵 Ti 制备 Al-Ti-B 中间合金时, TiB₂ 粒子的形貌随着反应温度的升高而发生明显变化。当反应温度为 850 °C 时, Al-Ti-B 中间合金中的 TiB₂ 粒子以大的聚集团形式存在, 而当反应温度升高到 1200 °C 时, TiB₂ 粒子的形貌转变为复杂的层片状和枝晶状。

关键词: Al-Ti-B 合金; TiB₂; 合成过程; 三维形貌

(Edited by YANG Hua)